Use of Swirl for Flow Control in Propulsion Nozzles

K. Knowles*
Royal Military College of Science, Shrivenham, England, United Kingdom
and
P. W. Carpenter†
University of Exeter, Exeter, England, United Kingdom

In certain off-design conditions it is desirable to vary the effective area of turbofan propulsion nozzles, e.g., to aid component matching or to reduce fan noise on approach. It has been suggested that the mass flux reductions associated with swirl could be used to achieve such variations. This paper addresses the questions of whether swirl can achieve the required mass flux reductions and whether this can be done with minimal thrust losses. A quasicylindrical theory is used to analyze the swirling flow, and comparisons are made with variable-area nozzles for specific case studies. For a low-specific thrust engine of high bypass ratio (BPR ≃ 12) the required fan nozzle mass flux reduction cannot be achieved using swirl, and in any case, swirl gives a far faster rate of decay of thrust with fan nozzle mass flux than does a variable-area nozzle. For a ducted fan of BPR ≃ 4, a 10% reduction in core nozzle mass flux can be achieved with swirl for slightly less thrust loss than with a variable-area nozzle. The swirl profile, however, needs to be carefully optimized.

Nomenclature

A = nozzle area
$A \ldots E$ = coefficients used in thrust equation, Eq. (4)
A_{eff} = effective nozzle area, Eq. (8)
A_{geom} = geometrical nozzle area
a = speed of sound
C_D = discharge coefficient, Eq. (8)
C_m = mass flux coefficient, Eq. (2)
C_n = impulse function, Eq. (3)
C_{st} = coefficient of specific thrust $= C_t/(C_{mc} + DC_{mf})$
C_t = coefficient of thrust, Eq. (1)
F_1, F_2 = coefficients used in thrust equation, Eq. (4)
h = enthalpy
$\dot{m}$ = mass flow rate
$\dot{m}_{\text{actual}}$ = actual mass flow rate
$\dot{m}_{\text{1Disen}}$ = one-dimensional, isentropic mass flow rate
p = presure
q = total velocity, $\sqrt{v^2 + w^2}$
Q = q/a_*
R_c = swirl velocity profile core radius, Fig. 2
R_e = outer radius of fan nozzle, Fig. 1
R_{ex} = outer radius of core nozzle, Fig. 1
R_{e2} = outer radius of fan stream at plane 2, Fig. 1
R_i = inner radius of fan nozzle, Fig. 1
r = radial coordinate
r' = radial coordinate variable
S, S_1, S_2, S_3, S' = swirl parameters, Eqs. (6) and (7)
s = entropy
t = thrust
V = v/a_*
V_F = v_F/a_{*c}
v = swirl velocity
v_F = flight velocity
W = w/a_*
w = axial velocity
x = fractional change in nozzle effective area under cruise conditions
y = fractional change in nozzle effective area between takeoff and cruise
Δm = $[(\dot{m}_{\text{cr}})_{\text{orig}} - (\dot{m}_{\text{cr}})_{\text{varied}}]/(\dot{m}_{cr})_{\text{orig}} = x$
γ = ratio of specific heats
ρ = density

Subscripts

a = ambient conditions
c = conditions in core stream
cowl = conditions on afterbody cowl, Fig. 1
cr = cruise conditions
e = conditions at fan nozzle lip
$e2$ = conditions on outside of fan stream at plane 2, Fig. 1
ex = conditions at core nozzle lip
f = conditions in fan stream
i = conditions on inside of fan nozzle
max = maximum value
orig = conditions before swirl is introduced (or v-a nozzle is closed)
to = takeoff conditions
varied = conditions after swirl is introduced (or v-a nozzle is closed)
0 = stagnation conditions
1 = fan nozzle exit plane, Fig. 1
2 = conditions in fan stream at core nozzle exit plane, Fig. 1
* = critical conditions

Presented as Paper 88-3003 at the AIAA/ASME/SAE/ASEE 24th Joint Propulsion Conference, Boston, MA, July 11-13, 1988; received Aug. 1, 1988; revision received March 6, 1989.

*Lecturer, Aeromechanical Systems Group. Member AIAA.
†Reader, School of Engineering. Member AIAA.

Introduction

With certain designs of turbofan aeroengines significant mass flux variations may occur between takeoff and cruise. For example, with low-pressure-ratio fans large fan mass flux changes occur between takeoff and cruise, leaving the core compressor operating at low efficiency in cruise or too close to surge during takeoff. In other designs, mass flux changes between takeoff and cruise can lead to problems with component matching and consequent thrust losses in cruise.

Such mass flux variations can be counteracted by adjusting the appropriate propelling nozzle area. Variable-area nozzles, however, are not readily accepted for civil engines because of

their weight and complexity. An alternative means of adjusting mass flux is the introduction of swirl into the propelling nozzle stream, possibly via variable-pitch swirl vanes. Before attempting to design such vanes, however, the viability of swirl needs to be assessed. It is necessary to determine whether the required mass flux variations can be achieved using swirl, how the thrust of such an arrangement compares with that of an equivalent variable-area nozzle, and which swirl profile gives the best performance.

To perform the assessment of swirl effects on nozzle performance a quasicylindrical theory has been developed for subcritical flows in annular, convergent nozzles[1] and for supercritical flows in circular, convergent nozzles.[2] This theory allows the calculation of radial pressure gradients due to swirl or nonuniform stagnation conditions[3] but not those due to streamline curvature. For the present comparative purposes, however, this is acceptable. Details of the theory have been given before, but a brief outline will be given for completeness.[1-3]

Following the theoretical development, two case studies that address two off-design problems are presented here. Swirl could be considered, though, to replace a variable-area nozzle in a noise reduction scheme such as that suggested by Adamson,[4] and the application of the analysis would be pertinent to a partial-swirl afterburner.[5,6]

Theoretical Basis

It is required to calculate, primarily, the effect of swirl on jet thrust. To this end an expression for thrust is derived for a short-cowl turbofan (Fig. 1) by applying a momentum balance to a control volume that extends from infinity upstream, laterally sufficiently far that ambient pressure can be considered to act on the side and downstream to plane 1 (see Fig. 1), then following the afterbody cowl and core nozzle exit. It is assumed that ambient pressure acts everywhere over plane 1 beyond the fan nozzle lip. When this is not the case, a postexit thrust component[7] exists, as discussed in Ref. 1; this will not be considered here. Similarly, effects of viscosity are not included in this analysis.

Nondimensional coefficients are now defined for thrust, mass flux, and impulse function:

$$C_t = t/(\rho_{*c} a_{*c}^2 \pi R_{ex}^2) \tag{1}$$

$$C_{mf} = 2\int_{R_i}^{R_e} \rho_f w_f r \, dr/(\rho_{*f} a_{*f} R_e^2) \tag{2}$$

$$C_{nf} = 2\int_{R_i}^{R_e} (p_f + \rho_f w_f^2) r \, dr/(p_{*f} + \rho_{*f} a_{*f}^2) R_e^2 \tag{3}$$

(and similarly for C_{mc} and C_{nc}). This leads to the equation for nondimensional net standard thrust[7]:

$$C_t = AC_{nc} + BC_{nf} + C(p/p_0)_{\text{cowl}} - V_F C_{mc} - V_F D C_{mf} - E \tag{4}$$

where

$$A = (\gamma_c + 1)/\gamma_c, \qquad C = (R_i^2 - R_{ex}^2)F_2/(p_a/p_0)_f E = F_2 R_e^2$$

$$B = (\gamma_f + 1)F_1, \qquad D = \gamma_f (a_{*c}/a_{*f}) F_1$$

$$F_1 = \frac{1}{\gamma_c}\left\{\frac{2}{\gamma_f + 1}\right\}^{\frac{\gamma_f}{\gamma_f - 1}} \left\{\frac{\gamma_c + 1}{2}\right\}^{\frac{\gamma_c}{\gamma_c - 1}} \left(\frac{p_a}{p_0}\right)_c \left(\frac{p_0}{p_a}\right)_f \left(\frac{R_e}{R_{ex}}\right)^2$$

$$F_2 = \frac{1}{\gamma_c}\left\{\frac{\gamma_c + 1}{2}\right\}^{\frac{\gamma_c}{\gamma_c - 1}} \left(\frac{p_a}{p_0}\right)_c \left(\frac{1}{R_{ex}}\right)^2$$

A similar expression holds for coplanar core and fan nozzles except that the term involving cowl pressure vanishes.

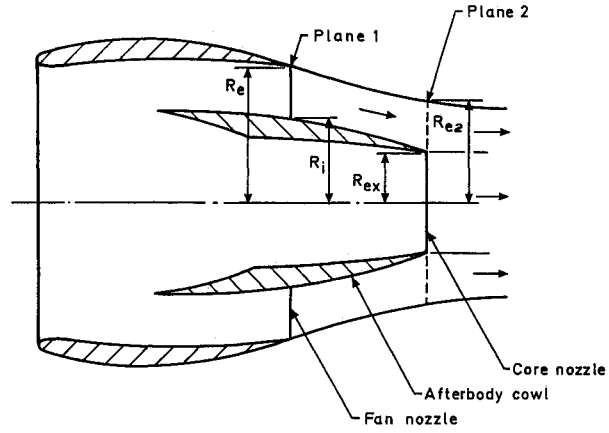

Fig. 1 Short-cowl turbofan geometry.

To evaluate the thrust coefficient it is thus necessary to know p/p_*, ρ/ρ_*, and w/a_* profiles at core and fan nozzle exit. These are all linked by the isentropic relations:

$$\frac{p}{p^*} = \frac{p}{p_0}\cdot\frac{p_0}{p^*} \text{ and } \left(\frac{p}{p_0}\right)^{\frac{\gamma-1}{\gamma}} = \left(\frac{\rho}{\rho_0}\right)^{\gamma-1} = 1 - \left(\frac{\gamma-1}{\gamma+1}\right)Q^2 \tag{5}$$

where $Q^2 = W^2 + V^2$. Axial and swirl velocity profiles can be linked using the Crocco vorticity theorem ($q \times \text{curl}\, q = \nabla h_0 - T\nabla s$). If a slender nozzle assumption is made and Crocco's expression is integrated across the nozzle exit plane then, for axisymmetric flow, this gives the nondimensional axial velocity as

$$W = (W_e^2 + S)^{1/2} \tag{6}$$

where

$$S = S_1 - S_2 + S_3$$

and

$$S_1 = 2\int_{r_1}^{R_e} (V_1/r_1')[\mathrm{d}(V_1 r_1')/\mathrm{d}r_1'] \, dr_1'$$

The S_2 involves the stagnation enthalpy profile and S_3 the entropy gradient, both of which will be taken to be zero for the present calculations (i.e., it is assumed that swirl will be introduced by nonrotating vanes).[1]

By applying conservation of mass to a streamtube between planes 1 and 2 (Fig. 1), conditions in the fan stream at plane 2 can be found from:

$$r_2 = \left\{R_{e2}^2 - 2\int_{r_1}^{R_e} (\rho_1 W_1/\rho_2 W_2) r_1' \, dr_1'\right\}^{1/2} \tag{7}$$

where

$$V_2 = V_1 r_1/r_2, \qquad W_2 = (W_{e2}^2 + S')^{1/2}$$

$$S' = 2\int_{r_1}^{R_e} (V_1 r_1'/r_2^2)\left[\mathrm{d}(V_1 r_1')/\mathrm{d}r_1'\right] dr_1'$$

(where h_0 and s gradients are again ignored). With fan stream flow calculated at plane 2, core nozzle conditions can then be found.

To determine engine thrust coefficient, for the general case of a short-cowl turbofan with swirl in both nozzles, the procedure is outlined in the following steps.

1) Specify swirl velocity profiles $V = V(r)$ at the exit of each nozzle.

2) From the specified fan nozzle back-pressure ratio p_a/p_{0f} calculate nozzle lip velocity Q_e using Eq. (5).

3) From steps 1 and 2 find W_e using $W_e^2 = Q_e^2 - V_e^2$.

4) Determine fan nozzle axial velocity profile using Eq. (6) together with steps 1 and 3. (Some typical velocity profiles are shown in Fig. 2.)

5) Calculate C_{mf} and C_{nf} using Eqs. (2) and (3) together with step 4 and Eq. (5).

6) Determine core nozzle lip conditions using Eqs. (7) and (5) to give gradients across the fan stream. It is assumed here that $Q_{e2} = Q_e$, but this is not a necessary condition.[1] [Note that solution of Eq. (7) is an iterative process.]

7) The C_{mc} and C_{nc} can now be calculated from the specified core nozzle swirl distribution, the lip back-pressure ratio (found from the specified p_a/p_{0c} and step 6), Eq. (5), and the core nozzle versions of Eqs. (6), (2), and (3).

8) The pressure acting on the afterbody cowl, which is required for Eq. (4), is taken as the average of those calculated at the inner ends of planes 1 and 2. It should be emphasized here that afterbody friction drag is not included in the present analysis.

If the nozzle pressure ratio is supercritical, i.e., greater than that which would produce a sonic axial velocity at the nozzle lip, then the procedure is as given except that $w_e = a_{*e}$ and similarly for the core.[2] Note that with a swirling fan stream and nonswirling, initially subcritical core flow the core nozzle can become choked as fan stream swirl increases.

Nonuniform entropy and stagnation enthalpy can be handled quite simply with this theory.[1] Equation (6) will have the terms S_2 and S_3 included in it; the expression for W_2 in Eq. (7) will be similarly modified, and the right-hand side of Eq. (5) (involving Q) will be amended. Postexit thrust[7] can also be determined if values are given to the local freestream pressures on the jet boundary at planes 1 and 2. Results are presented in Ref. 1.

Case Studies

Two case studies have been addressed here: a low-specific-thrust, fuel-efficient engine of bypass ratio (BPR) approximately 12, and a second-generation ducted fan of BPR approximately 4. In each case the requirement was to reduce the effective area of one of the nozzles in cruise. The approach, therefore, was to take the nozzle as originally designed (i.e., to leave unchanged the size and pressure ratio) and to apply swirl to the flow through it, analyzing the thrust and mass flux coefficients using the quasicylindrical theory. These results were then compared with a variable-area nozzle. Engine data are provided in Table 1. These case studies will now be discussed in more detail.

Low-Specific-Thrust Engine

This engine employs a low-pressure ratio fan that leads to a large change in fan nozzle mass flux between takeoff and cruise. This, in turn, means that the operating point moves as shown on the compressor map of Fig. 3. Hence, there is a need for a reduction in fan nozzle effective area between takeoff and cruise to avoid operating too near surge at takeoff and at too low a fan efficiency in cruise.

The effect of swirl on the fan nozzle mass flux coefficient is shown in Fig. 4 for three different swirl velocity profiles. The profiles used for this analysis are shown in Fig. 2a; for outer- and inner-biased profiles the minimum swirl velocity was zero for all calculations presented here. Both forced and free vortices have, however, also been analyzed; both were found to give results[1] that lie between those of the outer-biased and uniform swirl profiles when plotted against maximum swirl velocity as in Fig. 4. The use of maximum swirl velocity as a "swirl parameter" was discussed in Ref. 1: it is entirely an arbitrary choice driven by convenience, there is no compact "universal" swirl parameter for annular nozzle flows (a point corroborated by Dutton,[8] who only succeeded in finding empirically a nearly universal swirl parameter for mass flux coefficient in a variety of nozzles).

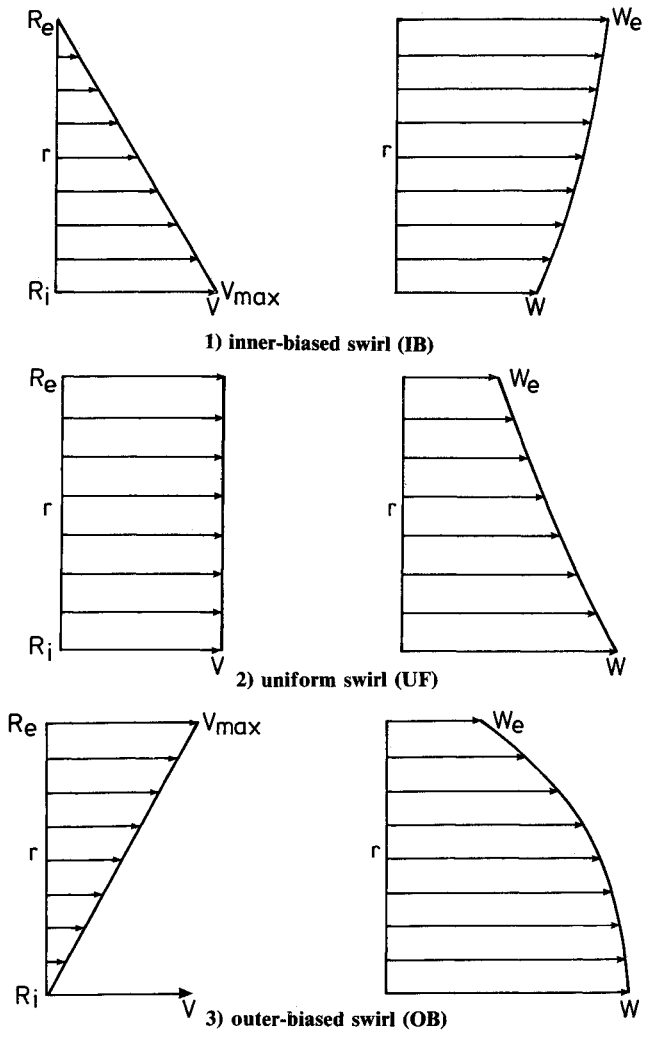

Fig. 2 Swirl velocity profiles and resulting axial velocity profiles (note that the scales are different for axial and swirl velocities).

Table 1 Engine data for case studies

Case	R_e	R_i	R_{ex}	Nozzle p.r. (p_0/p_a)[a] Takeoff Core	Takeoff Fan	Cruise Core	Cruise Fan	$\left(\frac{a_{*c}}{a_{*f}}\right)_{cr}$	M_F^b	$\left(\frac{A_{cr}-A_{to}}{A_{cr}}\right)^c$, % Core	Fan
Low-specific-thrust engine	1	0.6	0.35	1.2	1.2	1.89	1.89	1.5491	0.72	Small	−30
Second-generation ducted fan	1	0.6	0.6	1.5	1.75	2.0	2.6	1.6469	0.7	−10	Small

[a]$\gamma_f = 1.4$, $\gamma_c = 1.3$ in each case. [b]Approximate cruise Mach number. [c]Required change in nozzle effective areas.

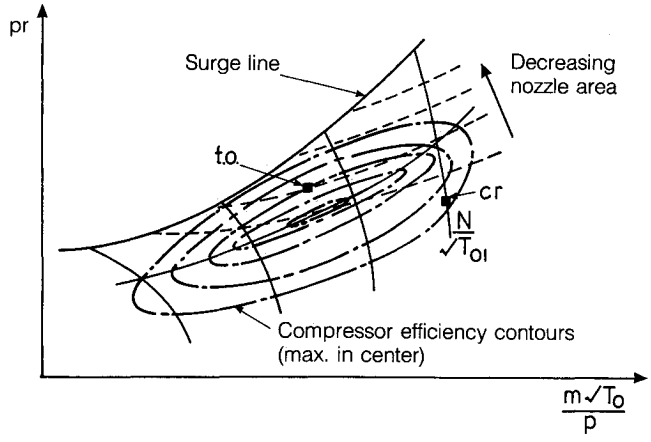

Fig. 3 Effect of change in fan nozzle effective area on compressor operating point.

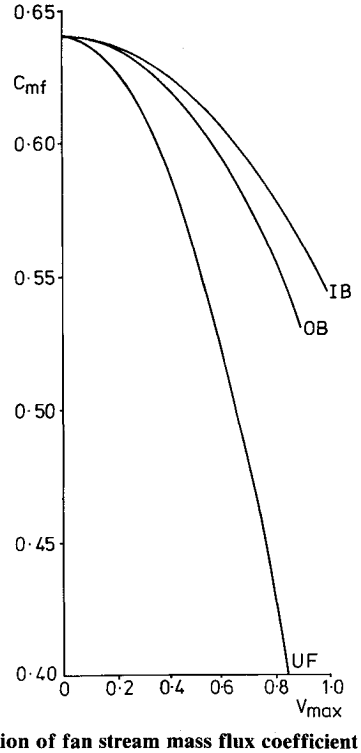

Fig. 4 Variation of fan stream mass flux coefficient with swirl (low-specific-thrust engine, $p_0/p_a = 1.89$). Key as Fig. 2a.

The effect of swirl on fan nozzle impulse function is similar to its effect on mass flux, and the net result is a decrease in thrust coefficient and specific thrust coefficient with increasing swirl level (Fig. 5). In this example, however, the core nozzle is choked under normal cruise conditions. Consequently, as swirl is introduced in the fan stream, the core nozzle becomes more underexpanded, but there is no effect on mass flux or exit impulse function. Further calculations were,

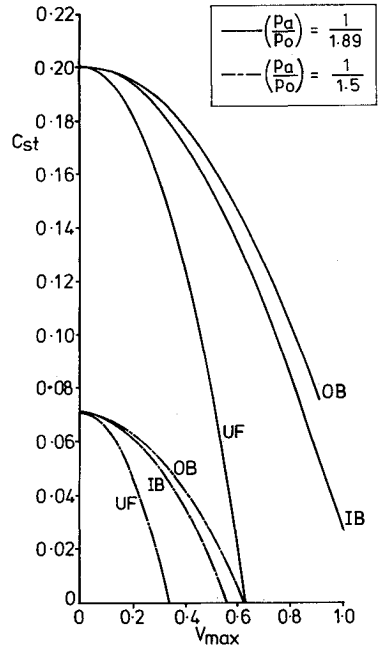

Fig. 5 Variation of specific thrust coefficient with swirl for two nozzle pressure ratios (the same pressure ratio is applied to both core and fan nozzle in each case). Key as Fig. 2a.

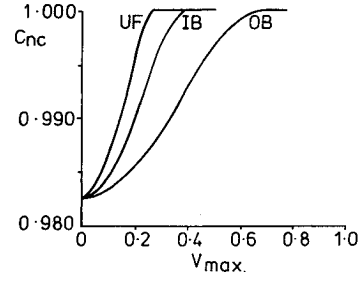

Fig. 6 Variation of core nozzle impulse function with fan nozzle swirl ($p_0/p_a = 1.5$ for both nozzles). Key as Fig. 2a.

therefore, performed with a subcritical pressure ratio (1.5) applied to both nozzles. The effect of fan stream swirl on core nozzle impulse function is shown in Fig. 6; C_{mc} follows similar curves and overall the specific thrust of the engine varies with swirl, as shown in Fig. 5. The curves are of a very similar shape to those obtained at the higher pressure ratio, although at a lower level of specific thrust and, hence, involving larger percentage changes for a given swirl increment. This may be because of the swirl parameter chosen (which does not scale with thrust level).

The very high bypass ratio used in these cases results in the core nozzle making a relatively small contribution to overall engine thrust. Consequently, the fan flow dominates and so further calculations were performed for lower bypass ratios at both of the stated nozzle pressure ratios to see whether swirling

the fan stream might offer benefits for such engines. In both cases, the same trend of specific thrust with swirl was found (Fig. 7).

The original subject of this case study, the engine described in Table 1, has been used for the comparison of swirl with a variable-area nozzle. Results are presented in Fig. 8 and suggest that swirl is not a viable alternative to a variable nozzle in this case, even if only small fan nozzle mass flux reductions are required. It should be noted, however, that the relative weights of the variable-area nozzle and swirl vanes are not included in this analysis.

Second-Generation Ducted Fan

The requirement here for a reduction in core nozzle effective area of 10% between takeoff and cruise (see Table 1) was to counteract the change in effective area that would otherwise occur and cause problems with the matching of internal components. This matching problem was found by the designers to lead to large thrust losses.

The cowling geometry assumed for this study was one with coplanar core and fan nozzles (see Fig. 9). This leads to a modification of the expression for thrust given in Eq. (4): the term involving cowl pressure vanishes. The analysis used in this case is as described previously except that, because the core nozzle pressure ratio is supercritical, nozzle lip conditions are set to critical (i.e., $W_{ex} = 1$). A further difference arises because of swirl being introduced into the core nozzle flow rather than the fan flow: there is no pressure gradient across the fan stream (in these calculations) affecting the core nozzle exit pressure.

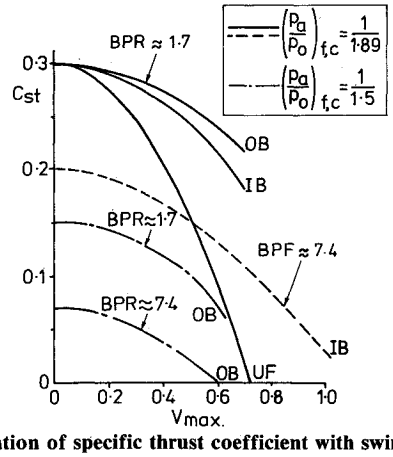

Fig. 7 Variation of specific thrust coefficient with swirl for two bypass ratios (BPR defined in cruise) and two nozzle pressure ratios (the same pressure ratio is applied to both core and fan nozzle in each case). Key as Fig. 2a.

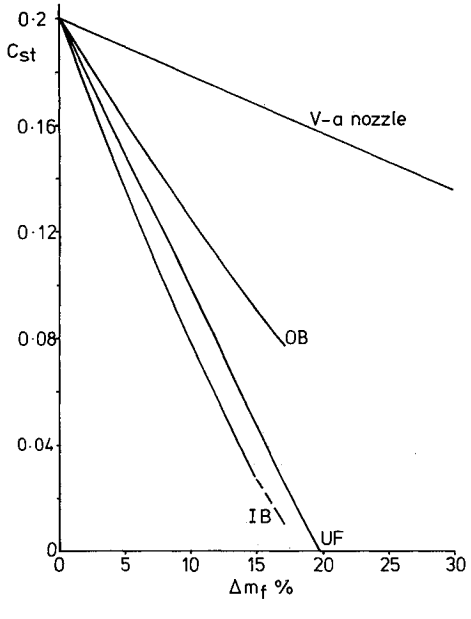

Fig. 8 Variation of specific thrust coefficient with fan nozzle mass flux change—comparison of swirl with variable-area nozzle for low-specific-thrust engine. Key as Fig. 2a.

Two families of swirl profile were assessed for this case study, the inner- and outer-biased profiles shown in Fig. 2b. In each case the maximum swirl velocity and the point at which the profile changes (R_c) could be varied. The effect of different swirl profiles, within these two families, on the core nozzle performance is shown in Fig. 10. Here, specific impulse function is plotted against mass flux coefficient for different values of R_c within each swirl family, the C_m variation being achieved by varying the maximum swirl velocity. Curves are plotted up to the onset of axial flow reversal (except the inner-biased profiles with $R_c = 0.4$–0.8, for which flow reversal occurs at values of C_m betwen 0.45 and 0.1). From this it can be seen that specific impulse functions in excess of unity are being predicted and that the more outer-biased the swirl profile, the higher the specific impulse for a given mass flux. The more highly outer-biased the swirl, however, the higher the maximum swirl velocity needed to obtain a given mass flux and, hence, the higher the mass flux coefficient at which flow reversal occurs. Thus, at low values of C_m inner-biased swirl offers the best performance; indeed, it is the only swirl option at such mass flux levels.

For the present case study the required core nozzle mass flux reduction equates to $C_{mc} = 0.91$ in cruise. It can be seen from Fig. 10 that this mass flux reduction can be achieved with any of the swirl profiles for which data are plotted. An outer-biased profile with $R_c = 0.8$, however, produces the highest specific impulse at this mass flux. More highly outer-biased swirl profiles will not attain this mass flux due to the prior onset of flow reversal. The optimum swirl profile for moderate mass flux reductions can be determined from Fig. 11, which plots the minimum value of C_m achieved for each outer-biased profile.

Having found C_{mc} and C_{nc}, engine thrust can be calculated using Eq. (4) (modified for coplanar nozzles) and the results compared with a variable-area nozzle. It should be recognized,

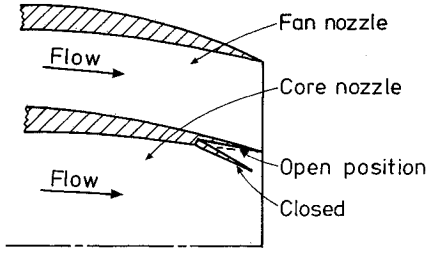

Fig. 9 Coplanar nozzles with "split-flap" variable-area core nozzle.

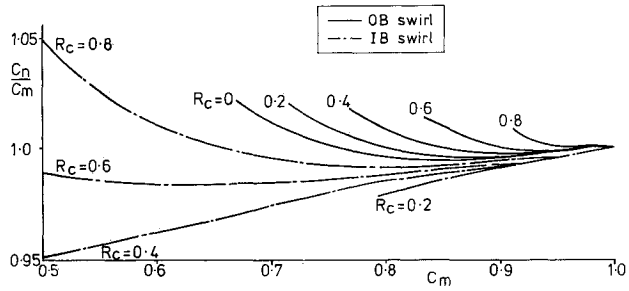

Fig. 10 Variation of specific impulse function with mass flux coefficient for the core nozzle of the second-generation ducted fan—effect of swirl profile. Key as Fig. 2b.

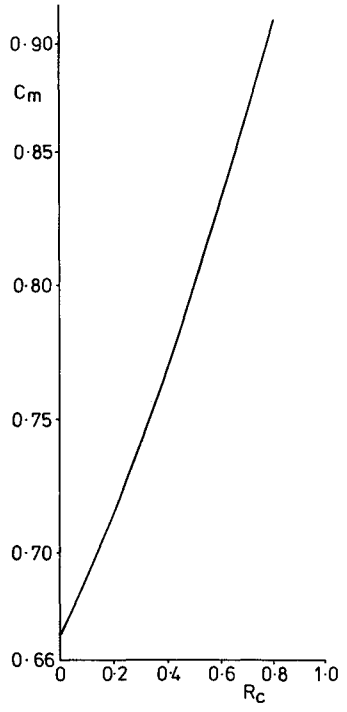

Fig. 11 Minimum mass flux coefficient achieved before axial flow reversal as a function of swirl profile core radius for OB swirl (see Fig. 2b); circular nozzle, $p_0/p_a = 2$.

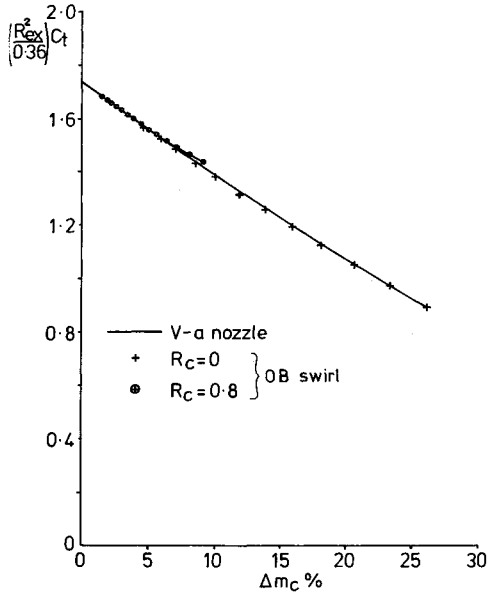

Fig. 12 Variation of normalized thrust coefficient with core nozzle mass flux reduction—comparison of OB swirl with variable-area nozzle for second-generation ducted fan. Key as Fig. 2b.

however, that reducing the core nozzle area will reduce the LP turbine pressure ratio and work output.[9] This in turn will decrease fan work and hence fan nozzle pressure ratio. Calculations of this process require knowledge of engine performance maps. In the absence of these, approximations have been made as follows. For a 10% decrease in core nozzle effective area it was assumed that the core nozzle stagnation pressure and temperature increased by 10%, while those in the fan nozzle decreased by the same amount. These changes in turn affect the ratio of critical sound speeds (a_{*c}/a_{*f}) and the nondimensional forward velocity (V_F).

At this point care should be taken over the interpretation of percentage changes. Those quoted in Table 1 are between takeoff and cruise, relative to the desired cruise condition (let us call this fraction y). Those referred to in the preceding paragraphs are between original and modified cruise conditions, relative to the original cruise value (let this fraction be x). To relate x and y to each other and to C_m, consider the definition of nozzle effective area:

$$\frac{A_{\text{eff}}}{A_{\text{geom}}} = C_D = \frac{\dot{m}_{\text{actual}}}{\dot{m}_{\text{1Disen}}} \tag{8}$$

If we drop the subscript "eff" for clarity in what follows we have

$$\frac{A_{\text{cr}}}{A_{\text{to}}} = \frac{1}{1-y} \quad \because y = \frac{A_{\text{cr}} - A_{\text{to}}}{A_{\text{cr}}}$$

which can be combined with Eq. (8) to give

$$\frac{1}{1-y} = \frac{(C_{mcr})_{\text{varied}}}{(C_{mcr})_{\text{orig}}} \frac{(A_{\text{geom}})_{\text{cr}}}{(A_{\text{geom}})_{\text{to}}}$$

[where $(C_D)_{\text{to}}$ is unity due to the one-dimensional nature of the present calculation]. We have defined x, however, to be

$$x = 1 - (\dot{m}_{\text{cr}})_{\text{varied}}/(\dot{m}_{\text{cr}})_{\text{orig}} \quad \therefore x = 1 - \frac{(C_{mcr})_{\text{varied}}}{(C_{mcr})_{\text{orig}}} \frac{(A_{\text{geom}})_{\text{cr}}}{(A_{\text{geom}})_{\text{to}}}$$

Thus, $x = 1 - (1-y)^{-1}$, i.e., a value of y of -10% equates to a cruise mass flux reduction (x) of 9.09% and $y = -30\%$ gives $x = 23.08\%$. Note that for swirling flow $(C_m)_{\text{cr}}$ varies and A_{geom} is fixed, whereas a variable-area nozzle maintains the same value of $(C_m)_{\text{cr}}$. In both cases the product is the same and so the described changes in nozzle stagnation conditions apply equally to a variable-area nozzle or to the swirling case.

The variation of thrust with core nozzle mass flux can now be investigated for both swirl and the variable-area nozzle. Since core nozzle radius (R_{ex}) is a nondimensionalizing factor in C_t, this comparison must be made on the basis shown in Fig. 12, where the original core nozzle had a radius of 0.6 (in arbitrary units). From this it can be seen that swirl is a viable alternative to a variable nozzle in this case. Careful optimization of the swirl profile can even give slight thrust increases over the variable-area nozzle at particular mass flux levels.

Discussion

Using a quasicylindrical theory for inviscid nozzle flows it has been shown that mass flux reductions can be achieved using swirl with no loss of thrust (in certain cases) when compared with a variable-area nozzle giving the same mass flux reduction. Clearly, the absence of a variable-area nozzle mechanism is a benefit, but it must be realized that to achieve the desired mass flux variation (between takeoff and cruise) swirl needs to be "switched" on and off. This could be achieved by using variable-pitch turbine-exit guide vanes (since only core nozzle flows seem here to benefit from swirl) designed to act as deswirlers in their takeoff setting and as swirl vanes, producing the required swirl velocity profile, in cruise. This might entail a difficult compromise in the design of the swirl blades. However, for moderate core nozzle mass flux reductions highly outer-biased swirl profiles are the most promising; consequently, only an outer annulus of swirl vanes would be needed. It is also conceivable that some form of circulation control might be applicable to the swirl vanes. It should be noted that the swirl profiles specified here are at nozzle exit, at a lower radius than the swirl vanes that would, therefore, need to be designed for lower swirl velocities.

The two case studies presented here suggest that the use of swirl as a mass flow control mechanism has more potential in core nozzles than in fan nozzles. This raises the question of why this should be. The swirl profiles chosen for study in the

fan nozzle case are more "severe" than those applied to the core nozzle in the other case study. (The reason for this was the large fan nozzle mass flux reduction that was the original aim.) It might be felt that more highly outer-biased profiles should have been applied to the annular nozzle. The outer-biased profile already applied here, however, does not produce specific impulse functions in excess of 1 (by contrast with those applied to the core nozzle in the other case study), and more highly outer-biased profiles would be limited by flow reversal to even lower maximum values of C_n/C_m.

Another difference between the two case studies lies in the pressure ratio applied to the swirling nozzle flow. In the case of the fan nozzle this is just subcritical, whereas the core nozzle (in the other study), because of the lower ratio of specific heats there, is initially choked. As swirl level increases, the nozzle eventually unchokes. This accounts for some cusplike features in Fig. 10, but it is not felt that it provides an explanation of the better core nozzle performance. The difference is felt to be due primarily to the annular nature of the fan nozzle, since Ref. 1 showed such nozzles to be more dependent on swirl level than circular nozzles. To a certain extent this is supported by Dutton's results,[8] since he found a lower vacuum-stream efficiency for a plug nozzle than for a circular, convergent-divergent nozzle at the same swirl parameter and with the same (constant-angle) swirl profile. This alone does not account for the poor performance of swirl seen in Fig. 8: much of this is due to cowl pressure, which is reduced by swirl but unaffected by the variable-area nozzle.

The off-design performance problems addressed here are not the only potential applications for swirl as a mass flux controller in propulsion nozzles. In general, anywhere a variable-area nozzle is needed swirl could be considered. The approach would be to size the nozzle for the maximum effective area required and then introduce swirl whenever a reduction is needed.

In the case of an engine with afterburning, other factors than those considered here may well determine the viability of swirl. Opening up the nozzle will remove the afterbody boattail; whether this increases aircraft drag depends on the effect of the swirling jet on the afterbody flow. Thrust augmentation levels of 10% imply nozzle effective area changes of 40%, which in turn would require strong swirl with large jet spreading rates, which may not be acceptable (because of interaction with aircraft surfaces). If a partial-swirl afterburner is to be employed,[5,6] then it may be of interest to use variable-pitch swirl vanes to achieve some measure of nozzle effective area reduction, possibly together with a simple, limited mechanical area variation.

If the core nozzle area is reduced on a three-spool turbofan, then the increased LP turbine back pressure leads to a reduction in fan speed.[9] This will reduce fan noise levels, which is of particular interest, since in modern high-bypass-ratio engines fan noise can be dominant, especially during approach. This may prove to be a useful application for swirl, since it only need be applied during landing. The noise reduction schemes proposed by Adamson,[4] however, involve maintaining high inlet Mach numbers through the fan during approach to reduce the forward propagation of fan noise. To achieve this involves increasing fan nozzle area which, if swirl were to be considered, would entail the use of swirl in the fan nozzle throughout the rest of the flight envelope. Also regarding engine noise reduction, it should be remembered that swirl can reduce shock-associated noise,[10] which may be of benefit in certain applications.

Conclusions

Swirling flow in propulsion nozzles has been studied as a possible mass flow control technique. Such mass flow control is needed in certain off-design conditions where variable-area nozzles would otherwise have to be employed.

In the case of a low-specific-thrust engine of BPR $\simeq$ 12, swirl in the fan stream gives a far faster rate of decay of thrust with fan nozzle mass flux than does a variable-area nozzle. Variants of this case study with lower bypass ratios and lower core nozzle pressure ratios showed no benefit for swirl. It is tentatively concluded that mass flow control with swirl in annular nozzles is unlikely to be feasible, particularly for short-cowl turbofans, although the relative weight penalty of a variable-area nozzle might change this in some circumstances.

For a ducted fan engine of BPR $\simeq$ 4, swirl can be used to control core nozzle mass flux with little or no loss of thrust over a variable-area nozzle. There are even slight thrust gains available if the swirl profile is optimized for the required mass flux reduction.

References

[1]Knowles, K. and Carpenter, P. W., "Subcritical Swirling Flows in Convergent, Annular Nozzles," *AIAA Journal,* Vol. 27, No. 2, 1989, pp. 184–191.

[2]Carpenter, P. W., "Supercritical Swirling Flows in Convergent Nozzles," *AIAA Journal,* Vol. 19, No. 5, 1981, pp. 657–660.

[3]Carpenter, P. W., "A General One-Dimensional Theory of Compressible Inviscid Swirling Flows in Nozzles," *Aeronautical Quarterly,* Vol. 27, Aug. 1976, pp. 201–216.

[4]Adamson, A. P., "Variable Thrust Nozzle for Quiet Turbofan Engine and Method of Operating Same," U.S. Patent 4,068,469, issued Jan. 17, 1978.

[5]Egan, W. J. and Shadowen, J. H., "Design and Verification of a Turbofan Swirl Augmentor," AIAA Paper 78-1040, July 1978.

[6]Hanloser, K. J. and Cullom, R., "Test Verification of a Turbofan Partial Swirl Afterburner," AIAA Paper 79-1199, June 1979.

[7]Mair, W. A. et al., "Definitions of the Thrust of a Jet Engine and of the Internal Drag of a Ducted Body," *Journal of the Royal Aeronautical Society,* Vol. 59, No. 536, Aug. 1955, pp. 517–526.

[8]Dutton, J. C., "Analysis of Swirling Nozzle Flow by a Time-Dependent Finite Difference Technique," Mechanical Engineering Dept., Texas A&M Univ., College Station, TX, Rept. TEES-TR-4990-84-01, Dec. 1984.

[9]Cohen, H., Rogers, G. F. C., and Saravanamuttoo, H. I. H., *Gas Turbine Theory,* 2nd ed., Longman, London, 1972.

[10]Carpenter, P. W., "A Linearized Theory for Swirling Supersonic Jets and its Application to Shock-Cell Noise," *AIAA Journal,* Vol. 23, No. 12, 1985, pp. 1902–1909.